Available online at www.sciencedirect.com
ScienceDirect
Journal of the European Ceramic Society 27 (2007) 4125–4129
www.elsevier.com/locate/jeurceramsoc

Sintering and properties of lead-free (K,Na,Li)(Nb,Ta,Sb)O_3 ceramics

F. Rubio-Marcos *, P. Ochoa, J.F. Fernandez

Electroceramic Department, Instituto de Cerámica y Vidrio, CSIC, 28049 Madrid, Spain

Available online 6 April 2007

Abstract

Two different stoichiometric $(K_{0.44}Na_{0.52}Li_{0.04})(Nb_{0.86}Ta_{0.10}Sb_{0.04})O_3$ and non-stoichiometric $(K_{0.38}Na_{0.52}Li_{0.04})(Nb_{0.86}Ta_{0.10}Sb_{0.04})$ $O_{2.97}$ compositions were prepared by the conventional mixed oxide and carbonate route. Low temperature synthesis process at 700 °C for 2 h, and further attrition milling process resulted in agglomerated powder of 500 nm of primary particles in the range of 50–70 nm. The ceramics sintered at 1125 °C showed the highest densification that decreased for higher sintering temperatures. Non-stoichiometric composition densification process was assisted through the presence of a liquid phase that promotes grain growth and the appearance of a secondary ferroelectric phase with tungsten–bronze type structure. The samples showed a relaxor type behaviour that diminished because of the compositional homogeneity improvement of the liquid phase in the non-stoichiometric samples. The higher piezoelectric properties were obtained for the samples with high ferroelectric type dielectric constant versus temperature behaviour. In the non-stoichiometric samples piezoelectric constant d_{33} values reach ~200 pC/N.

Keywords: Sintering; Microstructure final; Piezoelectric properties; Perovskites; Lead free

1. Introduction

The search for alternative lead-free piezoelectric materials is now being focused on modified bismuth titanates,[1–3] alkali niobates and systems in which a morphotropic phase boundary, MPB, occurred. Among them $(Na_{0.5}K_{0.5})NbO_3$, KNN, has been considered a good candidate for lead-free piezoelectric ceramics because of its strong piezoelectricity.[4] KNN exhibits a MPB at around 50% K and 50% Na separating two orthorhombic phases and, as for lead titanate zirconate piezoceramics (PZT), an increase in properties for compositions close to this MPB.[4] However, the major drawback of KNN ceramics is the need for special handling of the starting powders, sensitivity of properties to non-stoichiometry, and complex densification process.[5] The alkaline carbonates shown rather good water solubility and thus the water processing could introduce deviations in stoichiometry during the ceramic processing and could provoke ceramic degradation of the sintered samples. Excess of alkaline elements in the ceramic samples easily reacts with the moisture in the air and shows deliquescence.[5] One of the reasons for the poor sinterability of the KNN system is the low melting point of $KNbO_3$,[6] approximately at 1058 °C, moreover alkaline metal elements that were included in these materials easily evaporated at high temperatures. The evaporation of one of the constituents of the MPB provoke thus a compositional fluctuation of the composition as occurred in well known piezoelectric perovskite systems as PZT[7] that resulted in poorer properties. The sinterability of these materials should be improved by sintering aids as CuO[5–8] because of its low melting point. The sintering aid enters in B composition of the perovskite structure and the A site vacancies thus suppresses the formation of the hygroscopic secondary product.[9]

Recently, it was reported exceptionally high piezoelectric properties in the system $(K,Na)NbO_3$–$LiTaO_3$–$LiSbO_3$[10] prepared by a complex processing method, with d_{33} values over 400 pC/N in textured ceramics. Similar composition with 4 mol% of Lithium and 10 mol% of tantalum substituted KNN ceramic prepared by simple pressureless solid state sintering without aid additives or special powder handling reach interesting properties with d_{33} ~160 pC/N without antimony.[11] In addition of the good electromechanical properties comparable to those obtained in hard PZT, two aspects need to be clarified in these materials[11]: how the proximity of ambient temperature to the tetragonal-orthorhombic phase transition temperature would affect high reported properties? and which effect originated the high dielectric losses that are sometimes observed in KNN based materials?

The aim of this work is to study piezoelectric ceramic based in such a system by the conventional mixed oxide and carbonate route. The effect of the A/B ratio was inves-

* Corresponding author.
E-mail address: frmarcos@icv.csic.es (F. Rubio-Marcos).

0955-2219/$ – see front matter © 2007 Elsevier Ltd. All rights reserved.
doi:10.1016/j.jeurceramsoc.2007.02.110

tigated concerning the sintering process and piezoelectric properties.

2. Experimental

Two different composition were studied in this work: stoichiometric $(K_{0.44}Na_{0.52}Li_{0.04})(Nb_{0.86}Ta_{0.10}Sb_{0.04})O_3$ and non stoichiometric $(K_{0.38}Na_{0.52}Li_{0.04})(Nb_{0.86}Ta_{0.10}Sb_{0.04})O_{2.97}$, hereinafter will be named as S and NS, respectively. Both compositions were prepared to evaluate the effect of the excess B sites ions (A/B = 0.94). The ceramics were prepared by solid state synthesis from K_2CO_3, Na_2CO_3, Li_2CO_3, Nb_2O_5, Ta_2O_5, and Sb_2O_5. The raw materials used are all of high-purity grade. In order to optimize the particle size distribution raw materials were separately ball milled of ZrO_2 for 2 h using ethanol as the medium. All of the starting materials were weighed according to the desired compositions and were attrition milled in ethanol for 3 h. The powders were calcined at 700 °C for 2 h and then were attrition milled again for 3 h and dried. Particle size and agglomeration state of calcined powder were evaluated by means of a particle size analyser, Malvern Instrument Ltd. Powder morphology was observed by Field Emission Scanning Electron Microscopy (FE-SEM), Hitachi S-4700. The powders were cold-isostatically pressed at 200 MPa and the obtained compacts were sintered between 1075 and 1175 °C for 2 h. At the maximum sintering temperature, sintering time of 8 h to evaluate grain growth were realized. The densities of the sintered samples were obtained by the Archimedes method. The sintered samples were then cut into disks, polished and electroded with silver pasted and cured at 700 °C for 15 min.

The calcined powders and sintered samples were characterized by X-ray diffraction analysis on a Siemens Kristalloflex using Cu Kα radiation and using Si (from Silicon) as the internal standard. Microstructure was evaluated on polished and thermally etched at 1000 °C for 5 min by using FE-SEM equipped with Dispersed Spectroscopy, EDS. The average grain size was determined using Fullmann's method. Dielectric properties were measured using an HP 4294A precision impedance analyzer in the temperature range of 30–600 °C, at 2 °C/min, and in the frequency range of 100–1 MHz. P–E hysteresis loops were determined by a Radiant Technologies Inc. hysteresis meter (RT 6000 HVS) at room temperature. Ceramic disks were poled silicon oil with a 40 kV/cm field. Piezoelectric constant d_{33} was measured by a quasi-static Berlincourt Meter. The electromechanical coupling coefficients were determined from resonance and antiresonance methods on the basis of IEEE standards by using an impedance analyzer (HP4294A) at room temperature.

3. Results and discussion

Fig. 1 shows the FE-SEM micrographs and the particle size distribution of the calcined powder NS. As it can be seen, the calcined powders were ~500 nm agglomerates formed by smaller plate-like particles ranging from 50 to 70 nm. Stoichiometric composition had similar morphology, particles size distribution and agglomeration state (not shown). The small particle size was attributed to the low temperature process and will

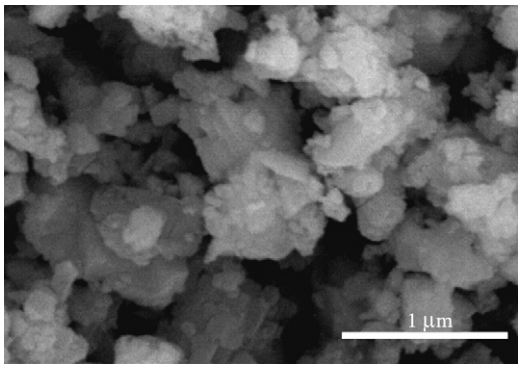

Fig. 1. FE-SEM micrographs of synthesized NS powders.

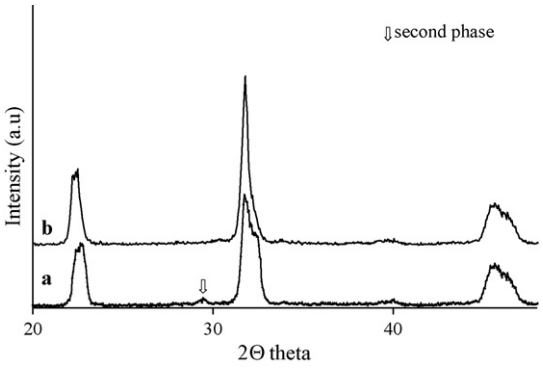

Fig. 2. X-ray powder diffraction (XPRD) of the S and NS calcinations at 700 °C for 2 h (a) NS and (b) S.

improve the reactivity of the powder. Regular synthesis process in KNN required temperatures higher as 850 °C for 5 h and twice calcinations.[5] The perovskite phase was formed and in NS composition only traces of Ta_2O_5 could be detected as a secondary phase by XRD, Fig. 2.

Fig. 3 shows the densities of the S and NS samples as a function of the sintering temperature. The density of all samples increased with sintering temperature up to 1150 °C, and then decreased for temperatures above this maximum soaking time. The evaporation of potassium oxide at high temperature was possibly the origin of such behaviour. The densities of the S samples were slightly higher, 4.69 g/cm^3 for 2 h and 4.69 g/cm^3 for 8 h. On the other hand, the densities of the NS samples were 4.63 g/cm^3 for 2 h and 4.66 g/cm^3 for 8 h. Sintered samples were

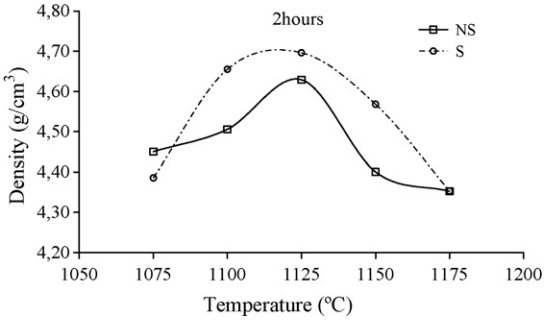

Fig. 3. Densification curves of S and NS ceramics vs. sintering time.

stored in water for 48 h and no differences were observed in dry sample weight and densities. In a similar way using a diamond disk and water as refrigerant sliced the samples and XRD of sliced surfaces does not show secondary phases related the formation of hygroscopic secondary products.

Fig. 4 shows the XRD profiles of S and NS ceramics after the sintering treatment at 1125 °C for 2 and 8 h. S samples XDR patterns revealed a pure perovskite material in the orthorhombic side of the MPB. By increasing the sintering time the tetragonal phase becomes more relevant as shown in Fig. 3b. However, NS samples with excess B sites cations showed a perovskite phase with a tetragonal crystalline symmetry and a secondary crystalline phase, Fig. 3c and d. In general, the formation of a solid solution between $(Na,K)NbO_3$–$LiTaO_3$–$LiSbO_3$ is extremely difficult to achieve due to the crystal structural differences between $KNbO_3$ and $NaNbO_3$ with a perovskite crystal structure and $LiTaO_3$ with a hexagonal pseudo-ilmenite crystal structure. Moreover, the solubility limit of $LiTaO_3$

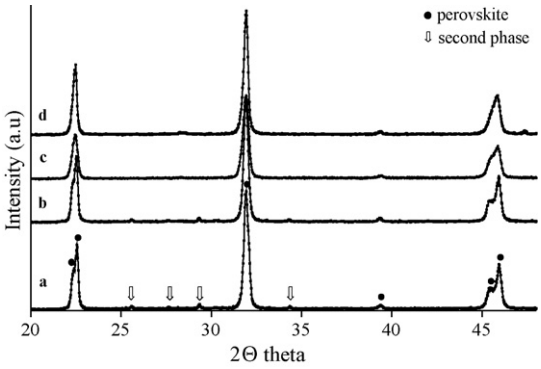

Fig. 4. X-ray powder diffraction (XPRD) of the S and NS sintered at 1125 °C (a) NS for 8 h; (b) NS for 2 h; (c) S for 8 h; (d) S for 2 h.

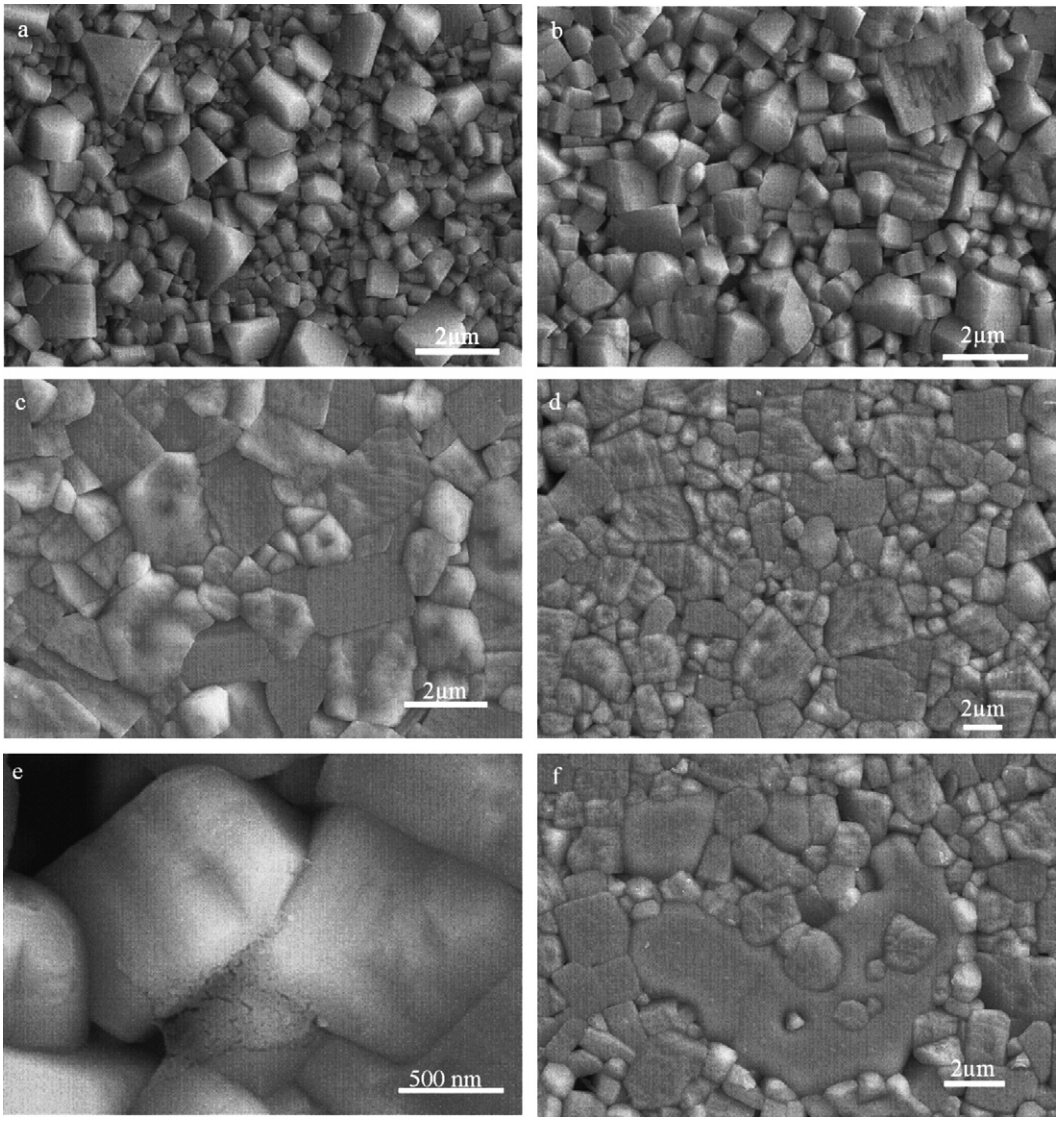

Fig. 5. FE-SEM photographs of ceramics sintered at 1125 °C (a) S 2 h; (b) S 8 h; (c) NS 2 h; (d) NS 8 h; (e) NS 2 h showing a detail of the liquid phase and (f) NS 2 h showing a detail of the second phase.

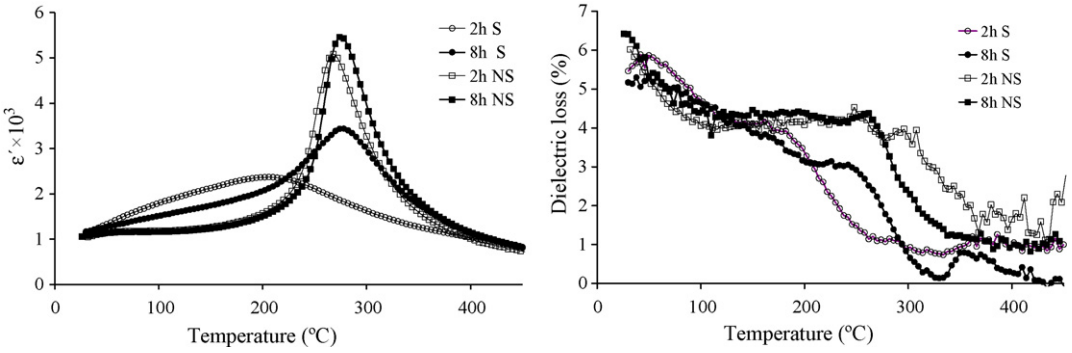

Fig. 6. The temperature dependence of the dielectric constant (ε_r) and loss at 1 MHz for unpoled in the samples S and NS sintered at 1125 °C for 2 and 8 h.

into (K,Na)NbO_3 is generally low. The solid solution moves from orthorhombic to tetragonal symmetry due to large distortion caused by Li^+. The presence of a secondary phase was found only in the non-stoichiometric composition and from the JPCDS file, the secondary crystalline phase was assigned to $K_3LiNb_6O_{17}$ with structure type tungsten–bronze.[12] KLN is a transparent oxide with a tetragonal tungsten–bronze structure (space group: P4bm; point group: 4 mm). The phase transition[13] ferroelectric–paraelectric occurs at Curie temperature of ∼420 °C.

Fig. 5 shows the FE-SEM micrographs of the S and NS samples sintered at 1125 °C for 2 and 8 h. The samples showed in general a bimodal grain size distribution. The average grain size of the S samples slightly increased from ∼0.64 ± 0.02 μm for 2 h to ∼0.89 ± 0.04 μm for 8 h. On the other hand, in the NS samples the average grain size was 1.44 ± 0.04 μm for 2 h, and ∼1.60 ± 0.07 μm for 8 h. In spite of the similar starting powder size and agglomeration state of both powders, the non-stoichiometric composition showed a higher grain growth. In the NS sintered at 1125 °C for 2 h samples, the presence of a secondary liquid phase was clearly shown in Fig. 4e. According to the phase diagram[6] the niobium excess forms a liquid at ∼1058 °C that could promote sintering with grain coarsening. Finally Fig. 4f shows the microstructure of the crystalline secondary phase as isolated grains of $K_3LiNb_6O_{17}$ in the SN matrix as confirmed by EDS. On the contrary, S composition under the same sintering conditions did not reveal the presence of liquid phase. Their existence could not be discarded because of the analogies between the densification curves of both series. The liquid phase did not promote exaggerated grain growth as expected and only seems to improve kinetically the mass transport during sintering.

The temperature dependence of the dielectric constant (ε_r) and dielectric loss at 1 MHz for unpoled samples is shown in Fig. 6. Dielectric constant versus temperature shows a peak related that was broader for the S samples. Meanwhile the 8 h sintered samples show similar maximum temperature, the 2 hours sintered S sample possess the broadest maximum at a temperature of ∼200 °C, indicating that the ferroelectric to paraelectric transition becomes diffusive. In addition to the typical frequency dependence of the dielectric maximum (not shown for clarity of the figure) the dielectric loss dependence shows a decrease in the transition indicating a relaxor like behaviour. The diffusiveness of the relaxor effect diminished with the grain size indicating that the liquid assisted mechanism promotes chemical homogeneity as the grain growth, however, the relaxor like behaviour if presented in all the studied samples. (NaK)NbO_3 ceramics generally show two phases transition temperatures,[11] that is, an orthorhombic to tetragonal phase temperature at 200 °C and tetragonal to cubic phase temperature of approximately 420 °C. In the current N and NS, the first phase transition occurs below 25 °C because the lithium addition stabilized the tetragonal phase. In addition, an increase of the dielectric losses is observed for the room temperature regimen that could be associated with such transition. Related to the second transition, Sb^{+5} and Ta^{+5} were found to shift the Curie temperature downward slightly and are expected to lead to higher level of electronegativity when compared to niobium, making the KNN-based perovskite more covalent in nature.[10] The fact that grain growth increased the transition temperature and reduced the diffusiveness indicated that the perovskite was compositionally inhomogeneous and the origin of the relaxor like behaviour could be attributed to fluctuation of A or B cation distribution even the cations were isovalent in such positions. Meanwhile relaxor behaviour was correlated with non-isovalent cation clustering in B position for PMN based ceramics (lead magnesium niobates),[14] and polar cluster like behaviour in Ti^{+4} substituted $BaZrO_3$ ceramics.[15]

Fig. 7 shows the P–E hysteresis loops of S and NS that show a typical ferroelectric polarization hysteresis loops at room temperature. Higher remnant polarization and coercive electric field values were obtained in NS samples (Table 1).

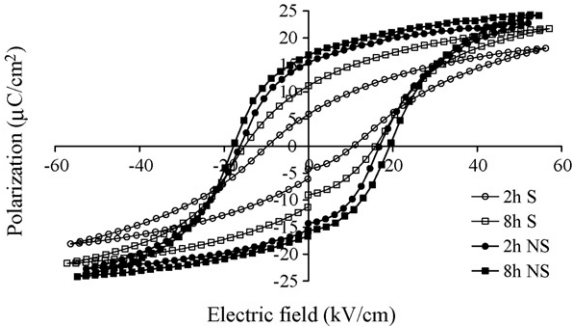

Fig. 7. P–E hysteresis loops of S and NS sintered at 1125 °C for 2 and 8 h.

Table 1
Ferroelectric and piezoelectric properties of the S and NS ceramics

	S		NS	
	2 h	8 h	2 h	8 h
δ (g/cm^3)	4.69	4.66	4.63	4.66
T_c (°C)	200	278	270	276
K_{33}^T	1286	1354	1258	1321
tg δ	0.041	0.038	0.033	0.028
d_{33} (pC/N)	54	103	170	195
d_{31} (pC/N) (–)	16.8	39.3	57.3	62.1
K_p	0.10	0.23	0.33	0.37
P_r (μC/cm^2)	6	11	15.5	17
E_c (kV/cm)	11	16	17	20

These ferroelectric parameters increased with sintering time in both compositions. The higher grain size, the homogeneous microstructure and tetragonal symmetry favour the ferroelectric response of these lead free piezoceramics. The liquid assisted sintering favoured the ferroelectric properties as was previously stated by the CuO addition.[5–8] The piezoelectric properties of poled S and NS ceramics were summarized in Table 1, show that the best properties were found in the NS composition related their higher homogeneity because of the grain growth. NS 8 h sintered samples possess a piezoelectric coefficient d_{33} near 200 pC/N and an electromechanical coupling coefficient $K_p = 38\%$.

4. Conclusions

Lead-free piezoceramics in the system (K,Na,Li)(Nb, Ta,Sb)O_3 had been prepared following a low temperature synthesis solid state route. The composition with excess B cations sintered in the presence of liquid phase that promotes grain growth and thus favours the solid solution of the perovskite. The samples showed a relaxor type behaviour that diminished because of the compositional homogeneity improvement that took place during the liquid phase assisted sintering in the non-stoichiometric samples. The relaxor like behaviour and the orthorhombic to tetragonal phase displace down to room temperature and were on the origin of the higher dielectric losses. Non-stoichiometric 8 h sintered samples shown higher ferroelectric and piezoelectric properties with $P_r \sim 17\ \mu C/cm^2$, $E_c \sim 20$ kV/cm and $d_{33} = 195$ pC/N.

Acknowledgements

The Spanish CICYT under contract MAT2004-04843-C02-01 financially supported this work. F. Rubio-Marcos was supported by a grant from FPI-CAM-FSE program.

References

1. Jaffe, B., Cook Jr. and Jaffe, H., *Piezoelectric Ceramics*. Academic Press, London, New york, 1971, pp. 185-212.
2. Maeder, M. D., Damjanovic, D. and Setter, N., Lead free piezoelectric materials. *J. Electroceram.*, 2004, **13**, 385–392.
3. Villegas, M., Moure, C., Fernandez, J. F. and Duran, P., Preparation and sintering behaviour of submicronic $Bi_4Ti_3O_{12}$ piezoceramics. *J. Mater. Sci.*, 1996, **31**(4), 949–955.
4. Egerton, L. and Dillon, D. M., Piezoelectric and dielectric properties of ceramics in the system potassium–sodium niobate. *J. Am. Ceram. Soc.*, 1959, **42**(9), 438–442.
5. Matsubara, M., Yamaguchi, T., Sakamoto, W., Kikuta, K., Yogo, T. and Hirano, S., Processing and piezoelectric properties of lead-free (K,Na)(Nb,Ta)O_3 ceramics. *J. Am. Ceram. Soc.*, 2005, **88**, 1190–1196.
6. Irle, E., Blachnik, R. and Gather, B., The phase diagrams of Na_2O and K_2O with Nb_2O_5 and the ternary system Nb_2O_5–Na_2O–Yb_2O_3. *Thermochim. Acta*, 1991, **179**, 157–169.
7. Fernandez, J. F., Moure, C., Villegas, M., Durán, P., Kosec, M. and Drazic, G., Composicional fluctuations and properties of fine-grained aceptor-doped PZT ceramics. *J. Eur. Ceram. Soc.*, 1998, **18**, 1695–1705.
8. Takao, H., Saoito, Y., Aoki, Y. and Hiribuchi, K., Microstructural evolution of crystalline-oriented $(K_{0.5}Na_{0.5})NbO_3$ piezoelectric ceramics with a sintering aid of CuO. *J. Am. Ceram. Soc.*, 2006, **89**, 1951–1956.
9. Kosec, M. and Kolar, D., On activated sintering and electrical properties of $NaKNbO_3$. *Mater. Res. Bull.*, 1975, **50**, 335–340.
10. Yasuyoshi, S., Hisaaki, T., Toshihiko, T., Tatsuhiko, N., Kazumasa, T., Takahiko, H., Toshiatsu, N. and Masaya, N., Lead-free piezocerámicas. *Nature*, 2004, **432**, 84–87.
11. Hollestein, E., Davis, M., Damjanovic, D. and Setter, N., Piezoelectric properties of Li- and Ta-modified $(K_{0.5}Na_{0.5})NbO_3$ ceramics. *Appl. Phys. Lett.*, 2005, **87**, 182905.
12. Junzo, T., Yosito, O., Masayuki, T., Masaji, S. and Shaw, E., The RMN study of Li ion motion in $K_3LiNb_6O_{17}$ and K_3LiTaO_{17}. *Jpn. J. Appl. Phys.*, 1981, **21**, 451–455.
13. Imai, K., Imaeda, M., Uda, S., Taniuchi, T. and Fukuda, T., Homogeneity and SHG properties of K_3Li_{2-x} Nb_{5+x} O_{15+2x} single crystals grown by micro-pulling-down technique. *J. Cryst. Growth*, 1977, **177**, 79.
14. Noheda, B., Cox, D. E., Shirane, G., Gao, J. and Ye, Z. G., Phase diagram of the ferroelectric relaxor $(1-x)PbMg_{1/3}Nb_{2/3}O_3-xPbTiO_3$. *Phys. Rev. B*, 2002, **66**, 054104.
15. Maiti, T., Alberta, E., Guo, R. and Bhalla, A. S., The polar cluster like behaviour in Ti^{4+} substituted $BaZrO_3$ ceramics. *Mater. Lett.*, 2006, **60**, 3861–3865.